

## Feedback Estimators for Identifying Headway Distance and Velocity of Longitudinal Platoon Vehicles

Hironori SUZUKI<sup>a</sup>  
Takashi NAKATSUJI<sup>b</sup>

<sup>a</sup> School of Engineering, Nippon Institute of Technology, Saitama 345-8501, Japan

<sup>a</sup> Email: viola@nit.ac.jp

<sup>b</sup> Graduate School of Engineering, Hokkaido University, Hokkaido 060-8628, Japan

<sup>b</sup> Email: naka@eng.hokudai.ac.jp

**Abstract:** A dynamic feedback system is developed for estimating the headway distance and velocity in a longitudinal three-vehicle platoon. The estimation system is modeled using a particle filter (PF) and an unscented Kalman filter (UKF) that estimate them by measuring the acceleration rate and/or velocity of probe vehicle(s) in the platoon. State equations are defined as a discrete conservation equation of headway distance and velocity, whereas the measurement equation is based on a conventional car-following model. The UKF and PF have the advantage of avoiding first-order approximation when implementing a filtering process to increase the estimation accuracy. Numerical analyses using artificial simulated data as well as real car-following data showed that the PF and UKF reduce the estimation errors in most cases compared to conventional approaches such as an extended Kalman filter (EKF) or neural Kalman filter (NKF). This was significant especially in the headway estimation, where the accuracy of the EKF estimates was low.

*Keywords:* Vehicle Platoon, Particle Filter, Unscented Kalman Filter, Feedback Estimation

### 1. INTRODUCTION

A vehicle platoon is a system that consists of multiple car-following vehicles moving longitudinally on an arterial road or freeway corridor. Dynamic estimates of the headway distance and velocity in the platoon enable us to evaluate the risk of collisions and to mitigate this risk by control strategies such as informing or warning the drivers or by vehicle control.

To make the vehicle platoon safer, the accuracy in evaluating the risk of rear-end collisions is a key issue. Numerous theoretical and numerical studies have been carried out to assess the probability of rear-end collisions between two consecutive vehicles, namely a leader and a follower (Hiraoka et. al., 2012; Kitajima *et al.*, 2009). With the development of such risk evaluation methods, vehicles equipped with driving support systems based on state-of-the-art sensing technologies are expected to be capable of avoiding such rear-end collisions. However, it is not always easy to achieve a high level of safety, because implementing collision avoidance for a single vehicle will not always guarantee the safety of multiple vehicles.

Some studies have been performed to analyze the safety of a vehicle platoon based on traffic simulations coupled with car-following observation data. Galler and Asher (1995) found that vehicle platoon safety is sufficiently maintained if vehicle sensing data such as acceleration, velocity, and headway distance obtained by the leader are transmitted to 6 to 7 other vehicles in the platoon. Biswas *et al.* (2006) proposed vehicle-to-vehicle communication protocols for traffic safety enhancement. Simulation analysis showed that the proposed

algorithm using these protocols mitigates the risk of rear-end collision of a three-vehicle platoon system. Contet *et al.* (2007; 2012) tackled linear platoon control both by simulation and experimental analysis using test vehicles and a multiagent system. Yi and Chong (2005) proposed and evaluated a vehicle control algorithm to make a five-vehicle platoon safer and mitigate the risk of rear-end collision. Suzuki *et al.* (2011) revealed that the probability of rear-end collisions on a real arterial corridor propagates backwards as an amplified wave when the platoon consists mainly of passenger cars.

In a realistic situation, however, sensing data are not obtained in real time by all platoon vehicles, because vehicles are not all equipped with a data-collection systems that can measure velocity and headway distance. Although Farrelly and Wellstead (1996) attempted to estimate lateral velocity of a vehicle by measuring the longitudinal velocity, their method is limited to single vehicles not platoons. Also, the control strategy proposed by Yi and Chong (2005) requires that the inter-vehicle spacing and the velocity of each vehicle be measured in real time. Since more time is required for vehicle-to-vehicle communication systems to spread to almost all vehicles on the road, an alternate approach is required to estimate such data indirectly from other vehicles that do have sensing systems.

The authors have been attempting to tackle this dynamic estimation problem using an extended Kalman filter (EKF) and a neural Kalman filter (NKF) in which the state and measurement equations are defined by artificial neural networks (ANNs), and to evaluate the efficiency and applicability of this approach through numerical analyses (Suzuki and Nakatsuji, 2011; Suzuki, 2012). However, the EKF and NKF have some difficulties to be overcome. The accuracy of estimates by the EKF deteriorates when calculating the derivatives of state and measurement equations. The NKF yields quite unstable and sensitive estimates with respect to the parameters of ANNs. Alternate approaches to the EKF and NKF have been required to make the estimation system more reliable and accurate.

The present research attempts to introduce additional feedback estimators such as a particle filter (PF) and unscented Kalman filter (UKF) and to evaluate whether the new estimators yield more accurate estimates than the conventional approaches, the EKF and NKF. Also, the evaluation is implemented not only by the artificial data but also by the real car-following data collected through a test track field test.

## 2. Theoretical Background of Feedback Estimators

In this section, the theoretical background of four estimators, the EKF, NKF, PF, and UKF, is briefly described based on Koabayashi (2012), Nishiyama (2011), Haykin (2001), Ikoma (2012), and Arulampalam *et al.* (2002).

### 2.1 State-Space Model

The following state and measurement equations are defined as the state-space model, which is required for feedback estimation:

$$\mathbf{x}_k = \mathbf{f}(\mathbf{x}_{k-1}) + \mathbf{v}_{k-1}, \quad (1)$$

$$\mathbf{y}_k = \mathbf{g}(\mathbf{x}_k) + \mathbf{w}_k, \quad (2)$$

where

$\mathbf{x}_k$  : state variables at time  $k$ ,

$\mathbf{y}_k$  : measurement variables,

$\mathbf{v}_k$  : system error,

$\mathbf{w}_k$ : measurement error,

$\mathbf{f}$ ,  $\mathbf{g}$ : possible non-linear functions.

Let  $\mathbf{y}_{1:k}$  and  $\mathbf{x}_{1:k}$  denote as a set of all available measurement and state variables up to time  $k$  given by:

$$\mathbf{y}_{1:k} \equiv \{\mathbf{y}_1, \mathbf{y}_2, \dots, \mathbf{y}_k\}, \quad (3)$$

and

$$\mathbf{x}_{1:k} \equiv \{\mathbf{x}_1, \mathbf{x}_2, \dots, \mathbf{x}_k\}. \quad (4)$$

The estimation problem is to calculate the posterior probability  $p(\mathbf{x}_k | \mathbf{y}_{1:k})$  when giving a set of all measurement  $\mathbf{y}_{1:k}$ . If measurement  $\mathbf{y}_k$  is available, the posterior is updated through the Baye's rule:

$$p(\mathbf{x}_k | \mathbf{y}_{1:k}) = \frac{p(\mathbf{x}_k | \mathbf{y}_{1,k-1}) \cdot p(\mathbf{y}_k | \mathbf{x}_k)}{p(\mathbf{y}_k | \mathbf{y}_{1,k-1})}. \quad (5)$$

Here,  $p(\mathbf{y}_k | \mathbf{x}_k)$  is a likelihood function which describes the likelihood of  $\mathbf{x}_k$  when giving the measurement  $\mathbf{y}_k$ .  $p(\mathbf{x}_k | \mathbf{y}_{1,k-1})$  is a prior probability of  $\mathbf{x}_k$  given by:

$$p(\mathbf{x}_k | \mathbf{y}_{1,k-1}) = \int p(\mathbf{x}_k | \mathbf{x}_{k-1}) \cdot p(\mathbf{x}_{k-1} | \mathbf{y}_{1,k-1}) d\mathbf{x}_{k-1}. \quad (6)$$

Also,  $p(\mathbf{y}_k | \mathbf{y}_{1,k})$  is defined as:

$$p(\mathbf{y}_k | \mathbf{y}_{1,k-1}) = \int p(\mathbf{y}_k | \mathbf{x}_k) \cdot p(\mathbf{x}_k | \mathbf{y}_{1,k-1}) d\mathbf{x}_k. \quad (7)$$

$p(\mathbf{x}_k | \mathbf{x}_{k-1})$  in (6) and  $p(\mathbf{y}_k | \mathbf{x}_k)$  in (7) can be given by the state and measurement equations (1) and (2).

There is a strong restriction that the posterior and prior probability density functions (PDF)  $p(\mathbf{x}_k | \mathbf{y}_{1:k})$  and  $p(\mathbf{x}_k | \mathbf{y}_{1,k-1})$  should be Gaussian in a conventional Kalman filter, whereas the Particle Filter (PF) does not require any assumptions or analytical functions for the PDFs.

## 2.2 Extended Kalman filter (EKF)

Although the functions  $\mathbf{f}$  and  $\mathbf{g}$  should be linear when applying a Kalman filter (KF), many estimation problems in the real world require non-linear functions in the state and measurement equations (1) and (2). To overcome this problem, the two equations are linearized and approximated as the following equations based on the first-order Taylor expansion:

$$\mathbf{x}_k \cong \mathbf{A}_{k-1} \mathbf{x}_{k-1} + \mathbf{p}_{k-1} + \mathbf{v}_{k-1}, \quad (8)$$

$$\mathbf{y}_k \cong \mathbf{C}_k \mathbf{x}_k + \mathbf{q}_k + \mathbf{w}_k, \quad (9)$$

where

$\mathbf{p}_k$ ,  $\mathbf{q}_k$ : constant vectors,

$\mathbf{A}_{k-1}$ ,  $\mathbf{C}_k$ : Jacobian matrices defined by

$$\mathbf{A}_{k-1} = \frac{\partial \mathbf{f}}{\partial \mathbf{x}}, \quad \mathbf{C}_k = \frac{\partial \mathbf{g}}{\partial \mathbf{x}}. \quad (10)$$

Denote  $\tilde{\mathbf{x}}_k$ ,  $\hat{\mathbf{x}}_k$ , and  $\mathbf{y}_k$  as the one-step prediction of state variable, optimal estimate, and real measurement, the feedback estimation is then implemented through the process

below:

$$\tilde{\mathbf{x}}_k = \mathbf{f}(\hat{\mathbf{x}}_{k-1}) + \mathbf{v}_{k-1}, \quad (11)$$

$$\tilde{\mathbf{y}}_k = \mathbf{g}(\tilde{\mathbf{x}}_k) + \mathbf{w}_k, \quad (12)$$

$$\hat{\mathbf{x}}_k = \tilde{\mathbf{x}}_k + \mathbf{K}_k (\mathbf{y}_k - \tilde{\mathbf{y}}_k). \quad (13)$$

Here,  $\mathbf{K}_k$  is the Kalman gain defined by the following equations:

$$\mathbf{M}_k^{xx} = \mathbf{A}_{k-1} \mathbf{P}_{k-1} \mathbf{A}_{k-1}^T + \mathbf{V}_{k-1}, \quad (14)$$

$$\mathbf{M}_k^{xy} = \mathbf{M}_k^{xx} \mathbf{C}_k^T, \quad (15)$$

$$\mathbf{M}_k^{yy} = \mathbf{C}_k \mathbf{M}_k^{xx} \mathbf{C}_k^T + \mathbf{W}_k, \quad (16)$$

$$\mathbf{K}_k = \mathbf{M}_k^{xy} (\mathbf{M}_k^{yy})^{-1}, \quad (17)$$

$$\mathbf{P}_k = \mathbf{M}_k^{xx} - \mathbf{K}_k \mathbf{C}_k \mathbf{M}_k^{xx}, \quad (18)$$

where

$\mathbf{V}_k, \mathbf{W}_k$ : covariance of system and measurement errors,

$\mathbf{M}_k^{xx}, \mathbf{P}_k$ : covariance of estimation errors  $\tilde{\mathbf{x}}_k$  and  $\hat{\mathbf{x}}_k$ , respectively.

### 2.3 Neural Kalman filter (NKF)

Although the EKF is well known as a semi-optimum estimator for nonlinear systems, the approximation in Equation (10) increases the estimation errors when applied to highly nonlinear system (Nishiyama; 2011). To avoid the Jacobian matrix calculation, an ANN is introduced to redefine Equations (1) and (2) without using any analytical equations.

Assuming that the ANN consists of three layers, the input, middle, and output layers, each entry of  $\mathbf{A}_{k-1}$  and  $\mathbf{C}_k$  is computed by

$$\frac{\partial z_r}{\partial z_p} = z_r (1 - z_r) \sum_q \left( W_{qr} \cdot \frac{2}{\mu_0} \cdot z_q (1 - z_q) \cdot W_{pq} \right), \quad (19)$$

where

$W_{pq}$ : connection weight from input to middle layers,

$W_{qr}$ : connection weight from middle to output layers,

$z_p$ : input to the ANN,

$z_q, z_r$ : outputs from middle and output layers,

$\mu_0$ : slope of sigmoid function that defines the output from each neuron.

Prior training of the ANN using a back propagation method enables us to compute  $\mathbf{A}_{k-1}$  and  $\mathbf{C}_k$  without calculating partial derivatives in Equation (10). The feedback estimation of NKF is implemented by following the same procedure as the EKF through Equations (11) to (18).

### 2.4 Particle Filter (PF)

The key idea of particle filter (PF) is to represent the required posterior PDF by a set of random samples with associated weights and to compute the estimates based on these samples and weights (Arulampalam *et.al.*; 2002).

Let  $\left\{ \left( \mathbf{x}_{1:k-1}^{(i)}, w_{1:k-1}^{(i)} \right) \right\}_{i=1}^M$  denote as a set of particles and its associated weights. It is assumed that  $\left\{ \left( \mathbf{x}_{1:k-1}^{(i)}, w_{1:k-1}^{(i)} \right) \right\}_{i=1}^M$  is given from the posterior PDF at time  $k-1$ . When giving the measurement  $\mathbf{y}_k$  at time step  $k$ , the PF is to compute and update the particles and weights from  $\left\{ \left( \mathbf{x}_{1:k-1}^{(i)}, w_{1:k-1}^{(i)} \right) \right\}_{i=1}^M$  to  $\left\{ \left( \mathbf{x}_{1:k}^{(i)}, w_{1:k}^{(i)} \right) \right\}_{i=1}^M$ .

The weight is updated through the appropriate process called Sequential Importance Sampling (SIS). The SIS generates the particles based on the proposal distribution  $q(\mathbf{x})$  which is different from the objective distribution  $p(\mathbf{x})$  and then gives each particle the appropriate weight so as to make the particles to be close to the objective PDF.

The update process of weight is given by:

$$\tilde{w}_k^{(i)} = w_k^{(i)} \frac{p\left(\tilde{\mathbf{x}}_k^{(i)} \mid \mathbf{x}_{k-1}^{(i)}\right) p\left(\mathbf{y}_k \mid \mathbf{x}_k^{(i)}\right)}{q\left(\tilde{\mathbf{x}}_k^{(i)} \mid \mathbf{x}_{1:k-1}^{(i)}, \mathbf{y}_{1:k}\right)} \quad (i = 1, 2, \dots, M). \quad (20)$$

The PF is the feedback estimator that theoretically places the random particles in the probability field to yield the accurate posterior PDF based on the Baye's theory (Ikoma; 2012). It is guaranteed that the estimates through the filtering process are suboptimal (Ikoma; 2012). The estimation process of PF is as follows:

1) Initial sampling: Generate the initial particles  $\hat{\mathbf{x}}_0^{(i)} (i = 1, 2, \dots, M)$  at  $k = 0$  from the initial probability density function  $p(\hat{\mathbf{x}}_0)$ .

2) Importance sampling: Generate one-step prediction of samples  $\tilde{\mathbf{x}}_k^{(i)}$  and  $\tilde{\mathbf{y}}_k^{(i)}$  based on the state and measurement equations:

$$\tilde{\mathbf{x}}_k^{(i)} = \mathbf{f}\left(\tilde{\mathbf{x}}_{k-1}^{(i)}\right) + \mathbf{v}_{k-1}^{(i)}, \quad (21)$$

$$\tilde{\mathbf{y}}_k^{(i)} = \mathbf{g}\left(\tilde{\mathbf{x}}_k^{(i)}\right) + \mathbf{w}_k. \quad (22)$$

3) Importance weight: Calculate the importance weight  $\tilde{w}_k^{(i)}$  for each sample by the following equation:

$$\tilde{w}_k^{(i)} = w_k^{(i)} \frac{p\left(\tilde{\mathbf{x}}_k^{(i)} \mid \mathbf{x}_{k-1}^{(i)}\right) p\left(\mathbf{y}_k \mid \tilde{\mathbf{x}}_k^{(i)}\right)}{q\left(\tilde{\mathbf{x}}_k^{(i)} \mid \mathbf{x}_{k-1}^{(i)}, \mathbf{y}_{1:k}\right)} \quad (i = 1, 2, \dots, M). \quad (23)$$

Larger weight is given to particles for which the prediction  $\tilde{\mathbf{y}}_k^{(i)}$  is closer to the actual measurement  $\mathbf{y}_k$ .

4) Resampling: The particle  $\tilde{\mathbf{x}}_k^{(i)}$  is updated into  $\hat{\mathbf{x}}_0^{(i)}$  in proportion to the importance weight  $\hat{w}_k^{(i)}$ .

5) Normalize weight: Normalize the importance weight to  $\hat{w}_k^{(i)}$  by

$$\hat{w}_k^{(i)} = \frac{\tilde{w}_k^{(i)}}{\sum_{j=1}^M \tilde{w}_k^{(j)}}. \quad (24)$$

6) Estimation: From the updated particles  $\hat{\mathbf{x}}_0^{(i)}$ , compute the estimate by

$$\hat{\mathbf{x}}_k \approx \frac{1}{M} \sum_{i=1}^M \hat{\mathbf{x}}_k^{(i)} \left( = \sum_{i=1}^M \hat{w}_k^{(i)} \tilde{\mathbf{x}}_k^{(i)} \right). \quad (25)$$

## 2.5 Unscented Kalman Filter (UKF)

The UKF is another of the family of *derivative-free* Kalman filters, which require no calculation of partial derivative of state and measurement equations (Haykin; 2001). The EKF provides the first-order approximation to the optimal estimates, whereas the UKF captures the posterior mean and covariance accurately to their second-order Taylor expansions using a minimal set of carefully chosen sample points called sigma points (Haykin; 2001).

The first step to apply the UKF is to generate the sigma point as

$$\sigma_{i,P} = \left( \sqrt{(N + \lambda) \mathbf{P}_k} \right)_i, \quad (26)$$

$$\hat{\Phi}_{0,k-1} = \hat{\mathbf{x}}_0, \quad (27)$$

$$\hat{\Phi}_{i,k-1} = \hat{\mathbf{x}}_{k-1} + \sigma_{i,P} \quad (i = 1, \dots, N), \quad (28)$$

$$\hat{\Phi}_{i,k-1} = \hat{\mathbf{x}}_{k-1} - \sigma_{i-N,P} \quad (i = N + 1, \dots, 2N), \quad (29)$$

$$\tilde{\Phi}_k = \mathbf{f}(\hat{\Phi}_{k-1}), \quad (30)$$

where

$\sigma_i$ :  $i$ -th column vector of the lower triangle matrix when applying the Cholesky decomposition to  $\mathbf{P}_k$ ,

$N$ : number of state variables,

$\lambda$ : scaling parameter.

One-step prediction of state variables and the error covariance are then given by

$$\tilde{\mathbf{x}}_k = \sum_{i=0}^{2N} h_i \tilde{\Phi}_{i,k}, \quad (31)$$

$$\mathbf{M}_k^{xx} = \sum_{i=0}^{2N} h_i \left[ \tilde{\Phi}_{i,k} - \tilde{\mathbf{x}}_k \right] \left[ \tilde{\Phi}_{i,k} - \tilde{\mathbf{x}}_k \right]^T + \mathbf{V}_{k-1}, \quad (32)$$

where  $h_i$  is the weight defined by

$$h_i = \frac{1}{2(N + \lambda)}. \quad (33)$$

The same procedure is applied to compute  $\tilde{\mathbf{y}}_k$ ,  $\mathbf{M}_k^{yy}$ , and  $\mathbf{M}_k^{xy}$  by defining the sigma vectors  $\tilde{\Psi}_k$  and  $\tilde{\Omega}_k$  as follows:

$$\sigma_{i,M} = \left( \sqrt{(N + \lambda) \mathbf{M}_k} \right)_i, \quad (34)$$

$$\tilde{\Omega}_{0,k-1} = \tilde{\mathbf{x}}_0, \quad (35)$$

$$\tilde{\Omega}_{i,k} = \tilde{\mathbf{x}}_k + \sigma_{i,M} \quad (i = 1, \dots, N), \quad (36)$$

$$\tilde{\Omega}_{i,k} = \tilde{\mathbf{x}}_k - \sigma_{i,M} \quad (i = N + 1, \dots, 2N), \quad (37)$$

$$\tilde{\Psi}_k = \mathbf{g}(\tilde{\Omega}_k), \quad (38)$$

$$\tilde{\mathbf{y}}_k = \sum_{i=0}^{2N} h_i \tilde{\Psi}_k, \quad (39)$$

$$\mathbf{M}_k^{yy} = \sum_{i=0}^{2N} h_i [\tilde{\Psi}_{i,k} - \tilde{\mathbf{y}}_k] [\tilde{\Psi}_{i,k} - \tilde{\mathbf{y}}_k]^T + \mathbf{W}_{k-1}, \quad (40)$$

$$\mathbf{M}_k^{xy} = \sum_{i=0}^{2N} h_i [\tilde{\Phi}_{i,k} - \tilde{\mathbf{x}}_k] [\tilde{\Psi}_{i,k} - \tilde{\mathbf{y}}_k]^T. \quad (41)$$

Again, the Kalman gain is computed by Equation (17) from the error covariance  $\mathbf{M}_k^{yy}$  and  $\mathbf{M}_k^{xy}$ . Also, the optimal estimate is updated through Equation (13). Finally,  $\mathbf{P}_k$  is computed by

$$\mathbf{P}_k = \mathbf{M}_k^{xx} - \mathbf{K}_k \mathbf{M}_k^{xx} \mathbf{K}_k^T. \quad (42)$$

### 3. State-Space Model for Vehicle Platoon

Assuming that three vehicles form a longitudinal platoon system, as depicted in Figure 1, the dynamics of headway distance and velocity of each platooned vehicle are defined as

$$\ell_k^i = \ell_{k-1}^i + [v_{k-1}^{i-1} - v_{k-1}^i] \Delta t, \quad (43)$$

and

$$v_k^i = v_{k-1}^i + a_{k-1}^i \Delta t, \quad (44)$$

where

$\ell_k^i$  : headway distance of vehicle  $i$  at time  $k$ ,

$v_k^i$  : velocity,

$a_k^i$  : acceleration rate.



Figure 1. Three-vehicle platoon

The acceleration rate in Equation (44) is given by a conventional car-following model, which is well known as the Gazis-Herman-Rothery (GHR) model (Rothery; 1998):

$$a_{k+T}^i = \alpha \frac{(v_k^i)^n}{(\ell_k^i)^m} [v_k^{i-1} - v_k^i], \quad (45)$$

where

$\alpha, m, n$  : model parameters,

$T$  : vehicle reaction time.

For simplicity, the reaction time is assumed to be zero, i.e.  $T = 0$ , under the assumption that errors due neglecting  $T$  will be minimized by the feedback process of the estimator. For the same reason, it is assumed that  $\alpha = m = n = 1$ .

Substituting Equation (45) into (44) redefines the velocity as

$$v_k^i = v_k^{i-1} + \alpha \frac{(v_{k-1}^i)^n}{(\ell_{k-1}^i)^m} [v_{k-1}^{i-1} - v_{k-1}^i] \Delta t. \quad (46)$$

Equations (43) and (46) are regarded as the state equations, whereas Equation (45) can be used as the measurement equation for the state-space model of a vehicle platoon. If velocity is also chosen as a measurement variable, the additional measurement equation is

$$v_k^i = v_k^i. \quad (47)$$

When assuming that the third vehicle is the only probe car, i.e. the only car equipped with a sensing system, the estimation problem is reduced to precisely estimating the state variables such as headway distance and velocity of the second and third vehicles by observing the measurement variables of acceleration and/or velocity of the third vehicle. When observing acceleration only, the state and measurement variables are:

$$\mathbf{x}_k = [\ell_2 \quad v_2 \quad \ell_2 \quad v_2]_{(k)}^T, \mathbf{y}_k = [a_3]_{(k)}^T, \quad (48)$$

otherwise,

$$\mathbf{x}_k = [\ell_2 \quad v_2 \quad \ell_2 \quad v_2]_{(k)}^T, \mathbf{y}_k = [a_3 \quad v_3]_{(k)}^T. \quad (49)$$

It is preferable that the velocity of the 1st vehicle is also added to the measurement variables. However,  $v_k^1$  is not included in the measurement variables in this analysis, but explicitly given to the platoon system since the transition of  $v_k^1$  is not described and modeled in the state equation.

#### 4. Numerical Analysis Using Artificial Data

##### 4.1 Preparing Artificial Data Sets and Scenarios

Artificial data is created and applied to evaluate the performance of the four feedback estimators: the EKF, NKF, PF, and UKF.

Given the velocity of the first vehicle of the platoon system, Equations (43) and (46) simulate the headway distance and velocity of the second and third vehicles to create “theoretical” data to be estimated. Then, the state-space model that adds the system and measurement errors in Equations (1) and (2) also simulates  $\ell_k^i$ ,  $v_k^i$ , and  $a_k^i$ . The simulated  $a_k^i$  and/or  $v_k^i$  that include the errors are assumed as the “observation” of measurement variables.

A three-vehicle platoon traveling at a steady speed of around 18 m/s is made to decelerate and come to a complete stop. This process is repeated nine times with random initial headway distance and velocity to create nine scenarios, AS1 to AS9. The initial headway distance and velocity for each scenario is given in Table 1.  $\Delta t$  is set to 0.1 s.

Table 1. Initial headway and velocity for nine artificial scenarios

	$\ell_2$ (m)	$v_2$ (m/s)	$\ell_3$ (m)	$v_3$ (m/s)	$v_0$ (m/s)		$\ell_2$ (m)	$v_2$ (m/s)	$\ell_3$ (m)	$v_3$ (m/s)	$v_0$ (m/s)	
AS1	25.6	15.0	13.4	13.6	16.8		AS6	25.6	15.0	13.4	13.6	17.5
AS2	28.2	16.1	22.0	15.9	17.5		AS7	21.6	16.2	30.8	16.1	17.5
AS3	21.6	16.2	30.8	16.1	16.8		AS8	25.6	15.0	13.4	13.6	16.8
AS4	28.2	16.1	22.0	15.9	16.8		AS9	28.2	16.1	22.0	15.9	16.8
AS5	21.6	16.2	30.8	16.1	16.8							

### 4.2 Conditions for Numerical Analysis

The number of neurons in the ANN model for the state equation is 4-4-4 for input, middle, and output layers, and 4-4-1 for the measurement equation, as depicted in Figure 2. The number of particles generated in the PF is gradually increased from 100 to 1000 in steps of 100 and is set to the number at which the best estimate is generated. The scaling parameter  $\lambda$  in the UKF is set to 10 for all estimations.

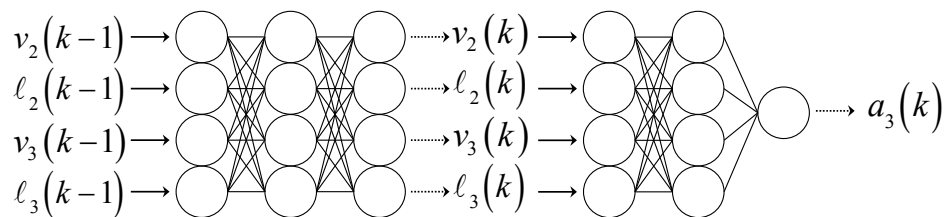


Figure 2. ANN models for state and measurement equations

### 4.3 Estimation Results by Measuring Acceleration Only

Figures 3 and 4 compare the estimates of headway distance and velocity in scenario AS2 between four feedback estimators, the EKF, NKF, PF, and UKF. Only one case out of nine scenarios is illustrated as an example. The statements “theoretical” in the legend means the theoretical value to be compared. The PF and UKF yield closer estimates to the target than the other estimators. In particular, in the headway and velocity estimation of the third vehicle, the PF and UKF significantly reduced the overestimation and underestimation that was seen in the EKF and NKF.

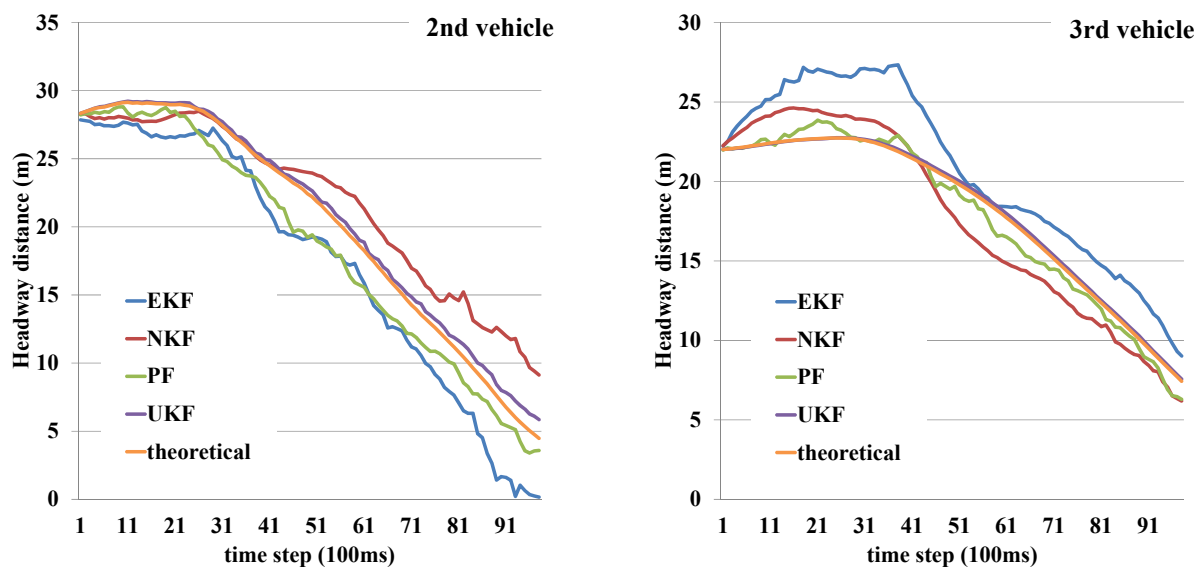


Figure 3. Estimates of headway distance in scenario AS2(measuring acceleration only)

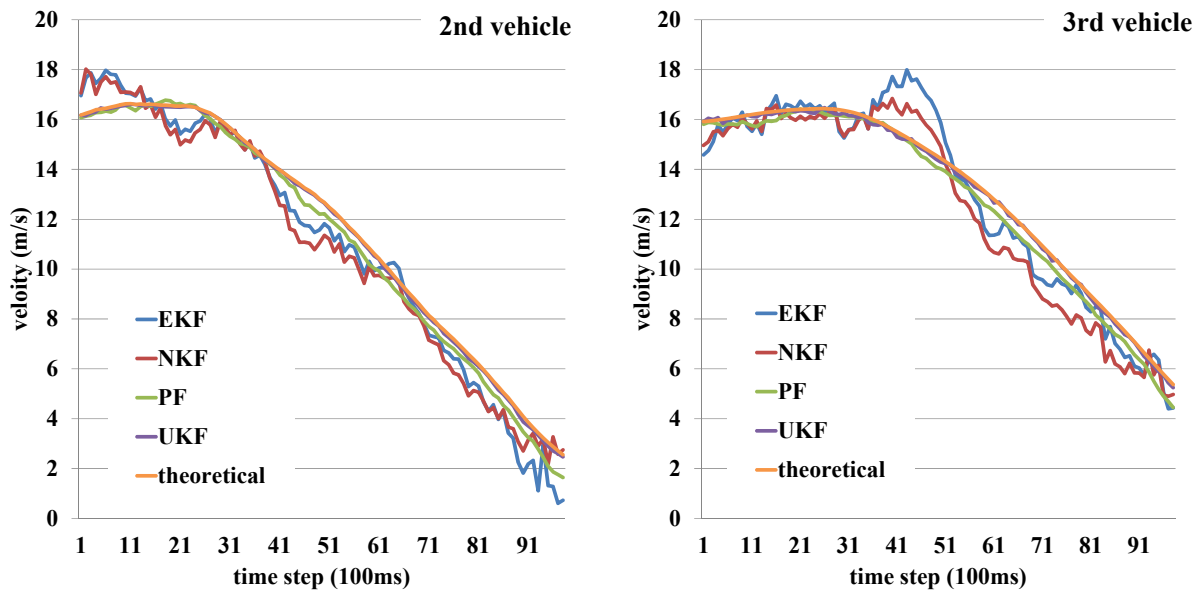


Figure 4. Estimates of velocity in scenario AS2 (measuring acceleration only)

Figures 5 and 6 depict the mean and standard deviation of root mean square error (RMSE) of the state variables for the total nine scenarios. The t-test shows that the mean RMSEs by the PF and UKF are statistically smaller than those by the other estimators for all state variables at more than 1 % confidence level. The UKF yields the best estimate and shows a higher accuracy even than PF at more than a 1% confidence level. This is more significant in the headway estimation of the third vehicle, where the conventional EKF did not show good performance.

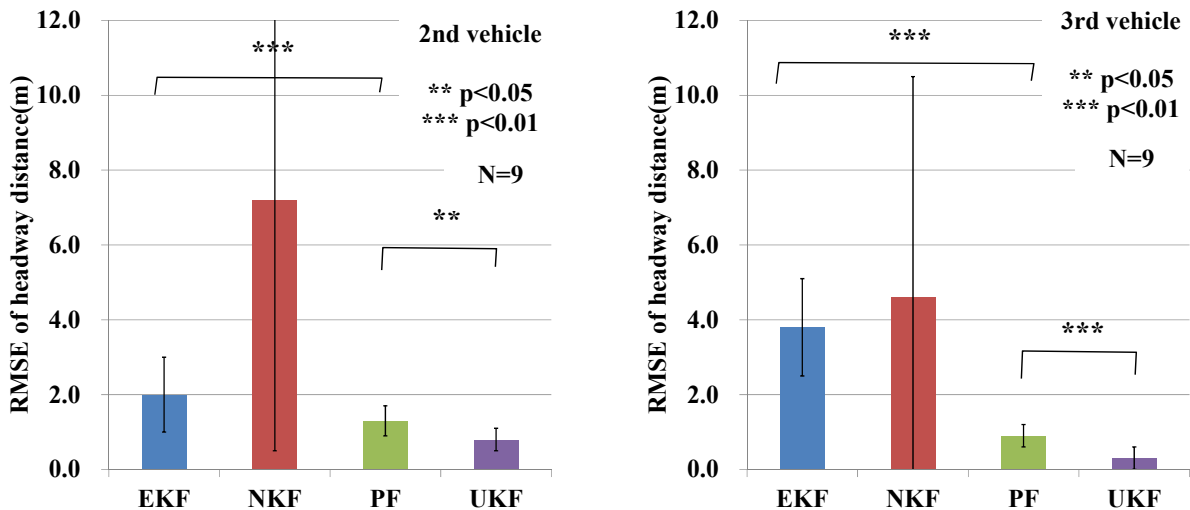


Figure 5. RMSE of headway distance estimations (measuring acceleration only)

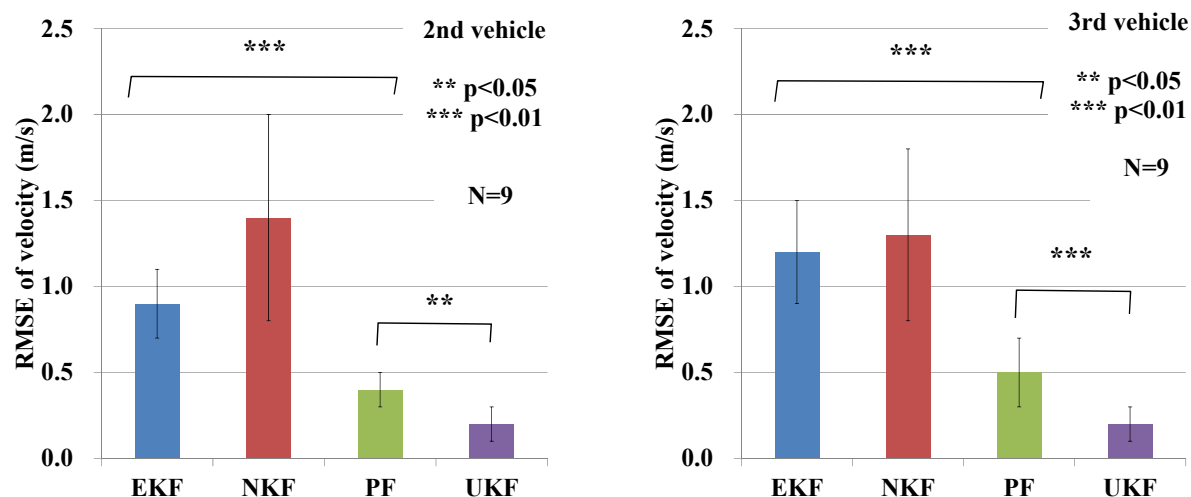


Figure 6. RMSE of velocity estimations (measuring acceleration only)

The estimate by the NKF is the worst for all state variables among the four estimators because the NKF is still sensitive to the parameters of the ANN. As shown in Table 2, however, the NKF outputs better estimates than the EKF in some scenarios for headway estimations. Although the NKF does not always yield inaccurate estimates, the NKF is more difficult to handle than the PF and UKF due to sensitivity to the parameters of the ANN.

Table 2. RMSE of all state variables for artificial nine scenarios (AS1~AS9).

RMSE of headway (m) (2nd vehicle)					RMSE of velocity (m/s) (2nd vehicle)				
	EKF	NKF	PF	UKF		EKF	NKF	PF	UKF
AS1	3.3	1.3	0.6	0.6	AS1	1.4	0.5	0.4	0.1
AS2	3.1	2.6	2.0	0.6	AS2	1.0	1.1	0.4	0.1
AS3	1.2	2.7	1.3	1.3	AS3	0.7	0.7	0.5	0.3
AS4	2.5	7.1	1.4	1.5	AS4	1.0	1.9	0.2	0.3
AS5	1.1	4.2	1.0	0.7	AS5	0.8	1.5	0.2	0.1
AS6	1.7	17.2	1.6	0.7	AS6	0.9	1.4	0.4	0.1
AS7	0.6	19.9	1.0	0.5	AS7	0.9	2.3	0.4	0.1
AS8	2.9	6.8	1.4	0.9	AS8	0.6	1.5	0.5	0.2
AS9	1.5	3.2	1.4	0.8	AS9	0.9	1.5	0.4	0.2
mean	2.0	7.2	1.3	0.8	mean	0.9	1.4	0.4	0.2
S.D	1.0	6.7	0.4	0.3	S.D	0.2	0.6	0.1	0.1
RMSE of headway (m) (3rd vehicle)					RMSE of velocity (m/s) (3rd vehicle)				
	EKF	NKF	PF	UKF		EKF	NKF	PF	UKF
AS1	4.8	0.8	0.7	0.3	AS1	0.8	0.6	0.8	0.1
AS2	2.9	1.8	0.7	0.2	AS2	1.0	1.1	0.4	0.1
AS3	1.5	1.5	1.1	0.3	AS3	1.0	0.8	0.6	0.3
AS4	2.5	1.3	1.3	1.1	AS4	1.3	1.8	0.3	0.4
AS5	4.1	4.6	0.9	0.2	AS5	1.8	1.7	0.2	0.2
AS6	4.9	1.7	0.5	0.2	AS6	0.8	1.1	0.4	0.1
AS7	3.8	7.6	1.4	0.3	AS7	1.4	1.9	0.5	0.1
AS8	5.9	2.5	0.9	0.3	AS8	1.1	1.4	0.7	0.2
AS9	3.6	19.2	0.7	0.2	AS9	1.2	1.6	0.5	0.2
mean	3.8	4.6	0.9	0.3	mean	1.2	1.3	0.5	0.2
S.D	1.3	5.9	0.3	0.3	S.D	0.3	0.5	0.2	0.1

#### 4.4 Estimation Results by Measuring both Acceleration and Velocity

The previous analysis showed that the PF and UKF provide the best performance among the four estimators, so that only the PF and UKF are accepted in the estimation where the velocity of a probe car is also chosen as a measurement variable in addition to the acceleration rate. The data sets and scenarios are the same as the analysis described in Section 4.1.

As an example out of nine scenarios, the performance of the PF and UKF in scenario AS9 is illustrated in Figures 7 and 8 in comparison with the case where no filter is applied. The superior performance of the PF and UKF are visible. Inaccurate estimate is observed in the no-filter case especially when estimating the headway distance of both the second and third vehicles. In contrast, The PF and UKF succeeded in minimizing the errors through the filtering process using the multiple particles and sigma points generated for those estimators.

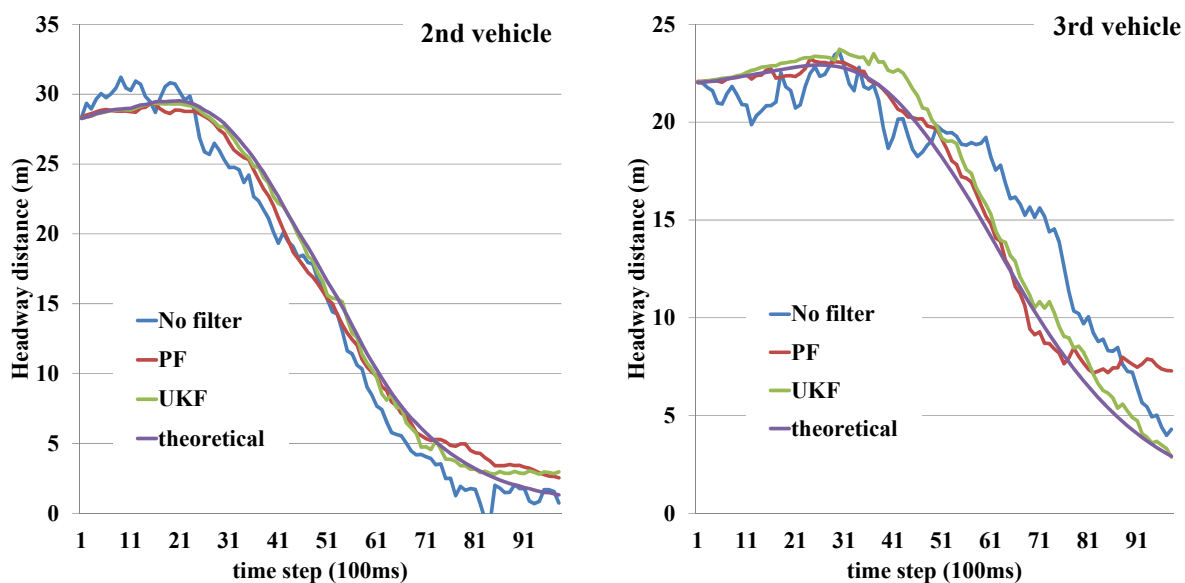


Figure 7. Estimates of the headway distance in scenario AS9 (measuring acceleration and velocity)

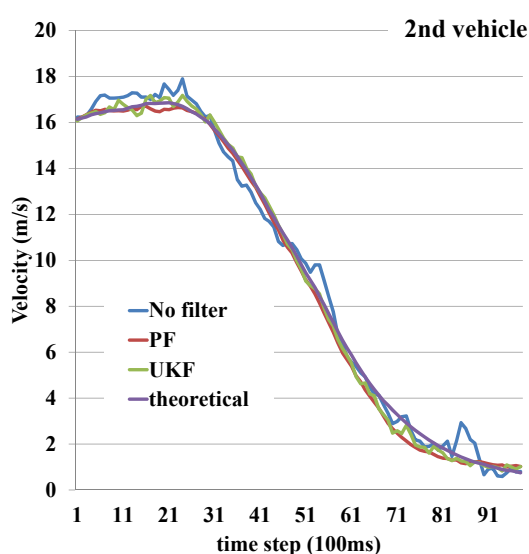


Figure 8. Estimates of the velocity in scenario AS9 (measuring acceleration and velocity)

The error statistics of headway and velocity estimations are depicted in Figures 9 and 10. The PF and UKF statistically show higher precision than the no-filter case at more than 1 % confidence level. Also, their variance of the errors are much smaller than the no-filter case. That is, both the PF and UKF had consistency lower errors with no statistical difference observed between them despite the UKF showing statistically higher accuracy than the PF in the case of measuring acceleration only. The better performance of the PF and UKF is still clear when using both acceleration rate and velocity as measurement variables. Note that one scenario of the UKF is excluded from the statistics due to an unexpected computation error in scenario AS5. It has not been confirmed, but it seems that the UKF may yield a slightly larger error when treating a state variable as also a measurement variable (i.e. the velocity of the third vehicle is a state variable to be estimated as well as a measurement variable).

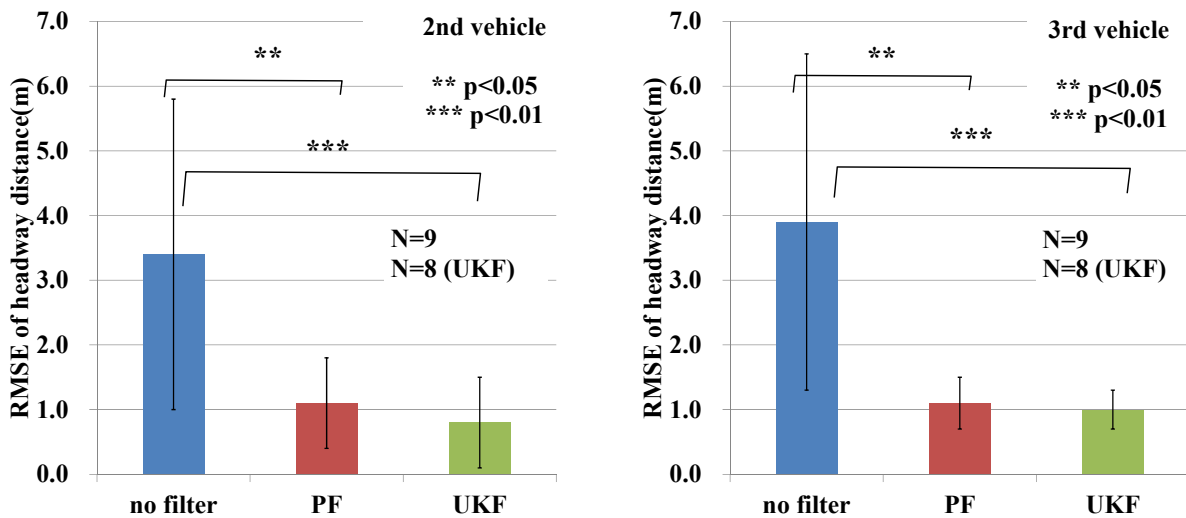


Figure 9. RMSE of headway distance estimations (measuring acceleration and velocity)

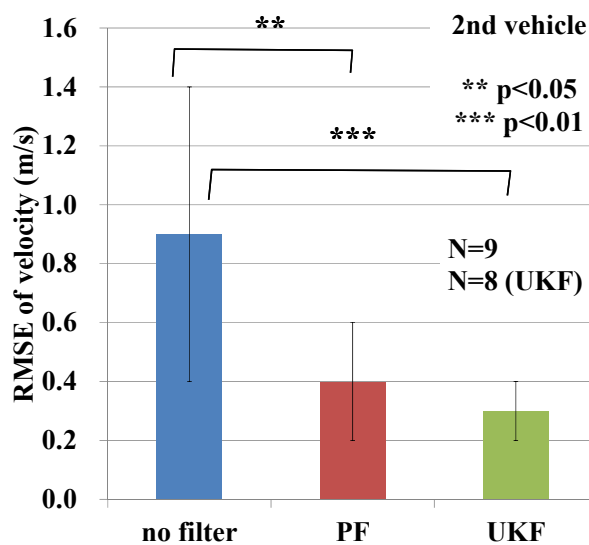


Figure 10. RMSE of velocity estimation (measuring acceleration and velocity)

## 5. Numerical Analysis Using Real Car-Following Data

### 5.1 Preparing Real Car-Following Data Set

Real car-following data including headway distance, velocity and acceleration rate of three vehicles were collected in a field test using a test truck of the Japan Automobile Research Institute (JARI). In the test, a three-vehicle platoon travelling at a steady speed of around 60 km/h was made to decelerate and come to a complete stop, and this process was repeated. The deceleration rate was random from 1 to 5 m/s<sup>2</sup>. Thirteen real-data scenarios (RS1 to RS13) which are suitable for the analysis were selected and used for the evaluation.

### 5.2 Estimation Results by Measuring Acceleration Only

As an example out of thirteen scenarios, Figures 11 and 12 compare the headway and velocity estimates of scenario RS4 among two estimators, PF,UKF and no-filter case. The statement “observed” in the legend means the real observed headway distance or velocity to be compared. PF and UKF yield more accurate estimates than no-filter case for all state variables. Especially in the headway estimation of 2nd and 3rd vehicles, PF and NKF reduced the unexpected under estimation that was seen in no-filter case.

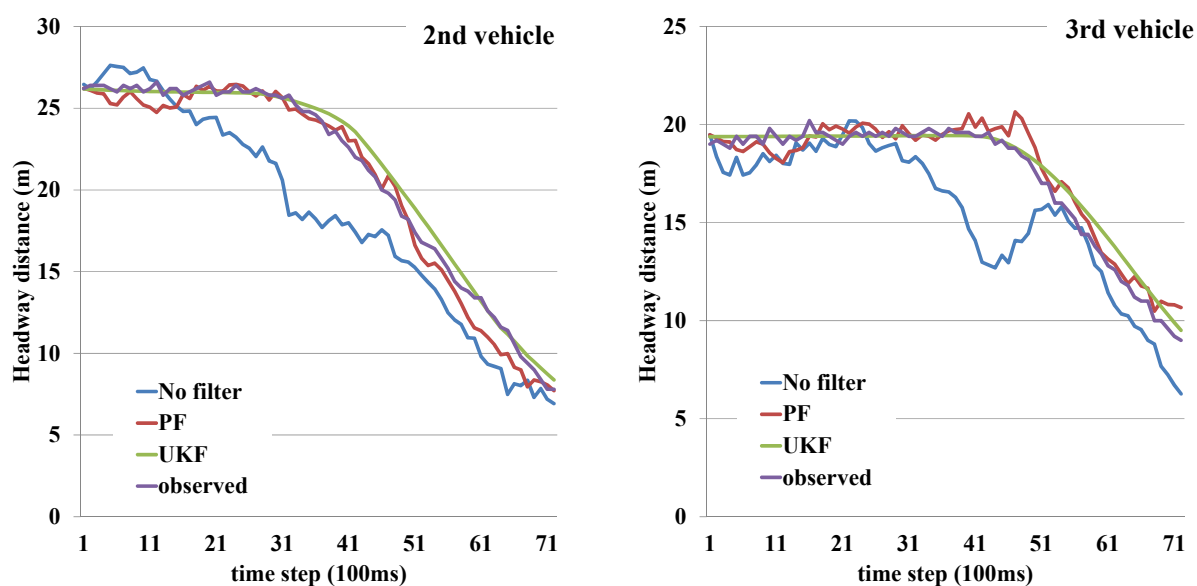


Figure 11. Estimates of headway distance in scenario RS4 (measuring acceleration only)

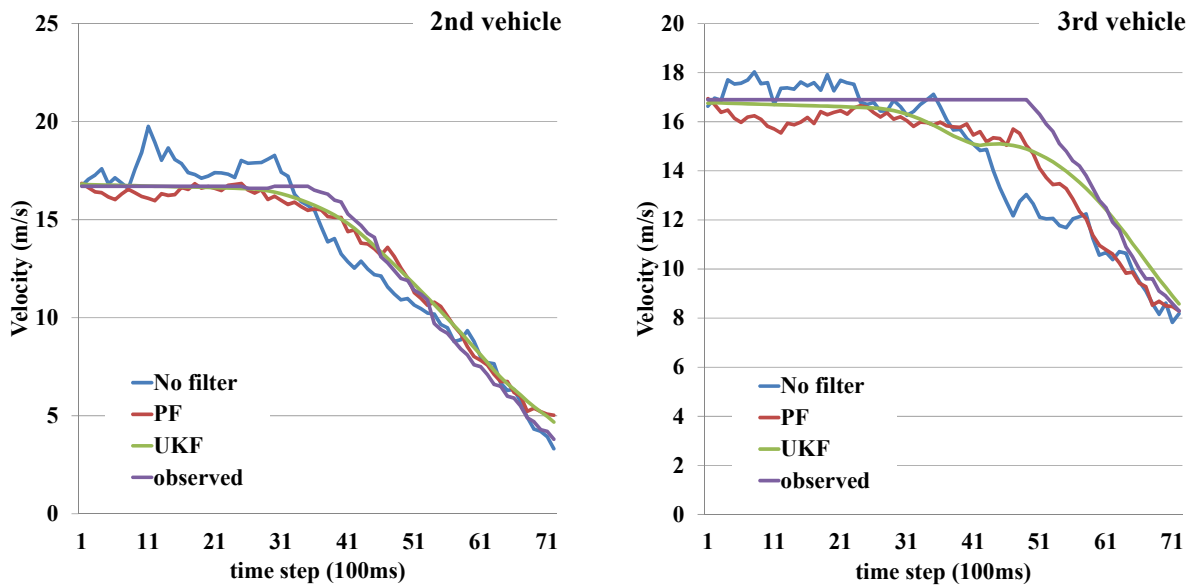


Figure 12. Estimates of velocity in scenario RS4 (measuring acceleration only)

Figures 13 and 14 depict the mean and standard deviation of root mean square errors (RMSE) of four state variables among thirteen scenarios. The t-test showed that mean errors of both headway estimates are statistically smaller than the no-filter case at 1% confidence level. The absolute error around 1 m, which is equivalent to the error by laser radar, is also acceptable as the satisfactorily level.

In the velocity estimations, however, no statistical difference is observed except the PF in the velocity estimates of 2nd vehicle although PF and UKF seem to decrease the mean errors. But, the absolute mean error around 0.8 to 1.2 m/s can be considered as the acceptable level for the collision risk evaluation.

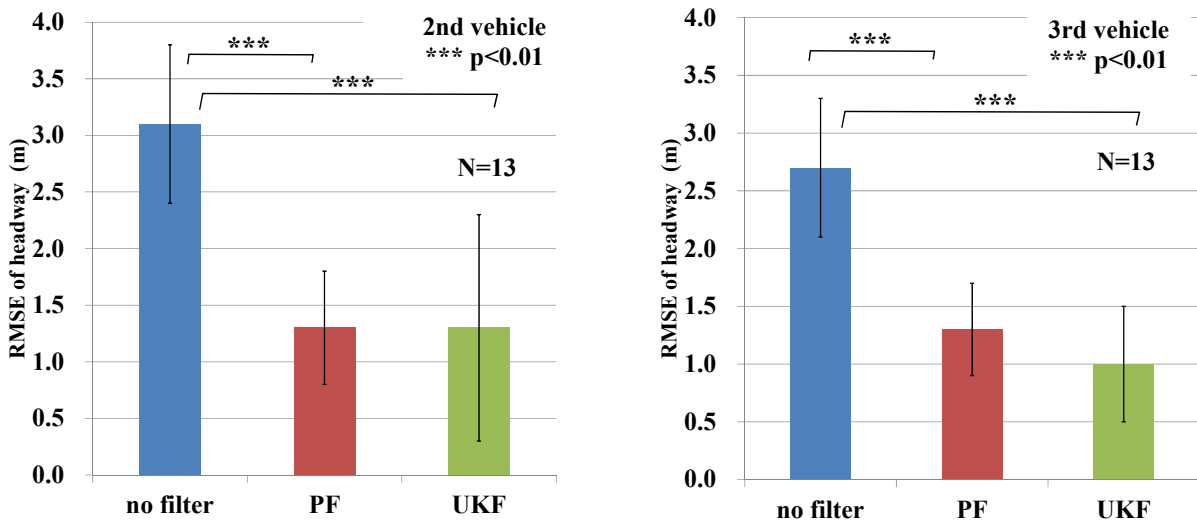


Figure 13. RMSE of headway distance estimations (measuring acceleration only)

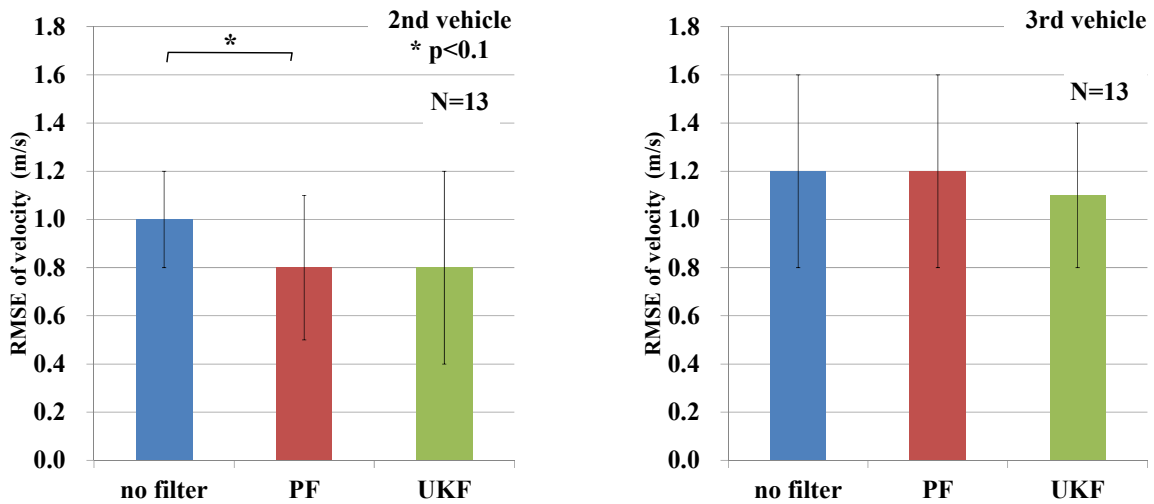


Figure 14. RMSE of velocity estimations (measuring acceleration only)

### 5.3 Estimation Results by Measuring both Acceleration and Velocity

An example of the Estimates by PF and UKF when measuring both acceleration and velocity are depicted in Figures 15 and 16 for the same scenario RS4. Although the PF and UKF still yield the outputs that are very close to the target, the precision is slightly worse compared to the case when observing acceleration only. In total, however, there is no difference in the mean estimation errors between the cases with and without the velocity observation, as depicted in Figures 17 and 18.

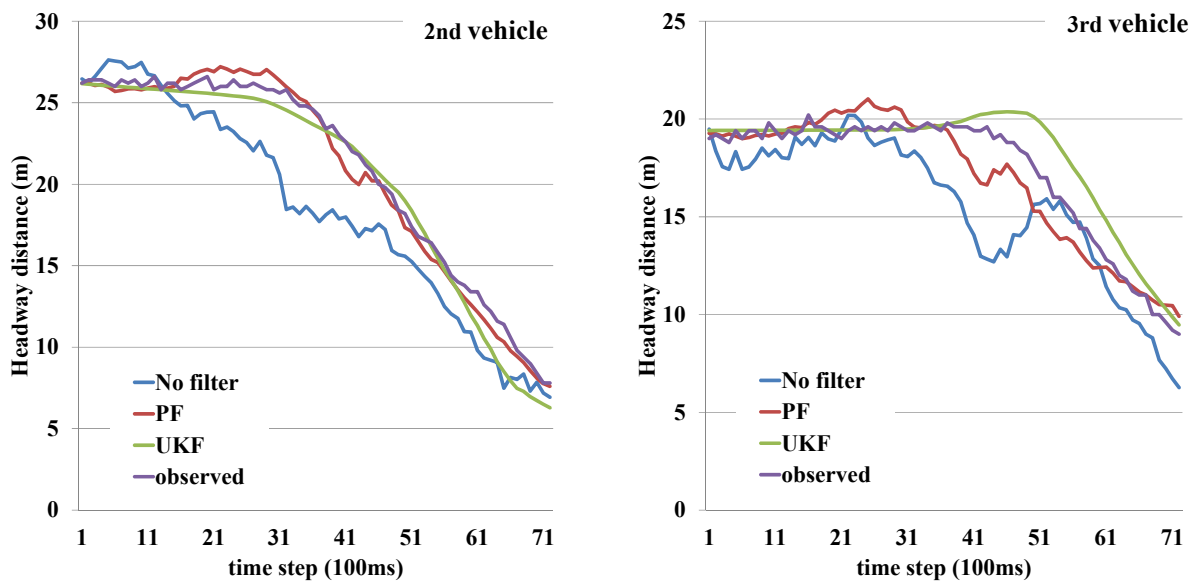


Figure 15. Estimates of headway distance in scenario RS4 (measuring acceleration and velocity)

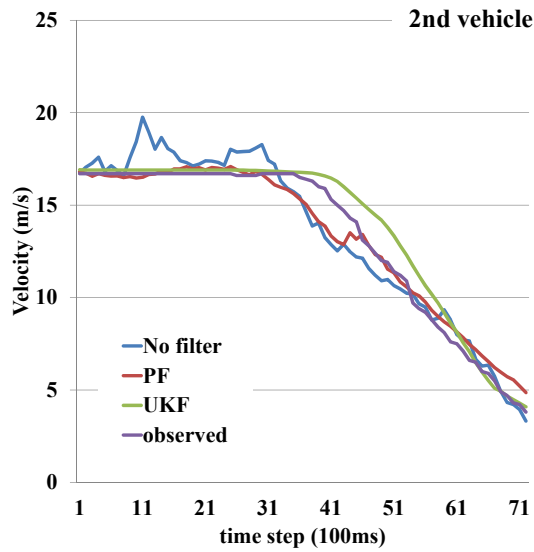


Figure 16. Estimates of velocity in scenario RS4 (measuring acceleration and velocity)

As illustrated in Figures 17 and 18, however, the mean errors by PF and UKF still remain small at the satisfactory levels for both headway and velocity estimations. Although there has been a variation in estimation accuracy depending on the car-following data or the measurement variables, acceleration and/or velocity at the 3rd vehicle are enough to estimate the headway which is difficult to be directly measured.

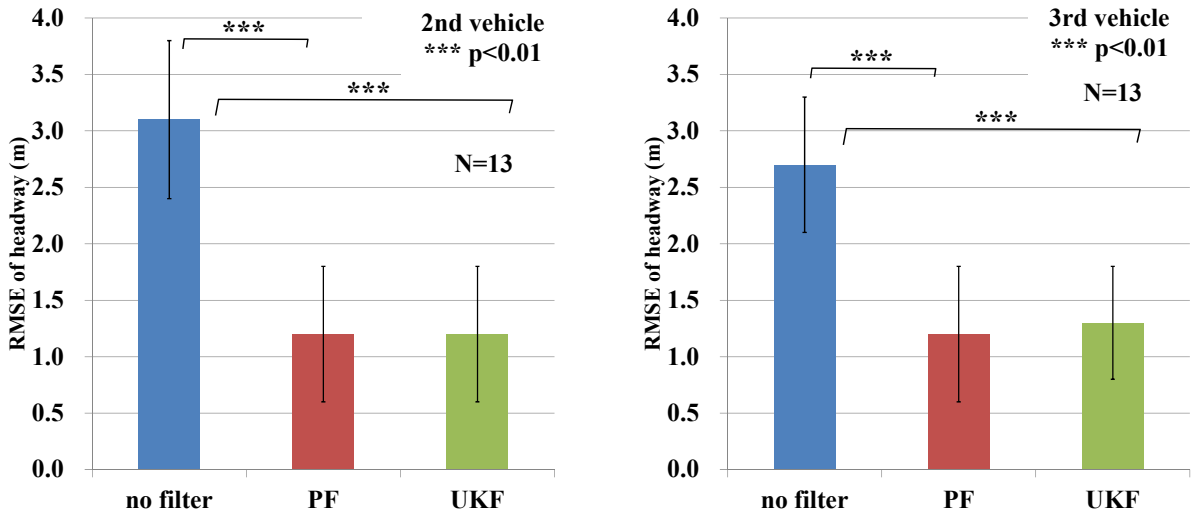


Figure 17. RMSE of headway distance estimations (measuring acceleration and velocity)

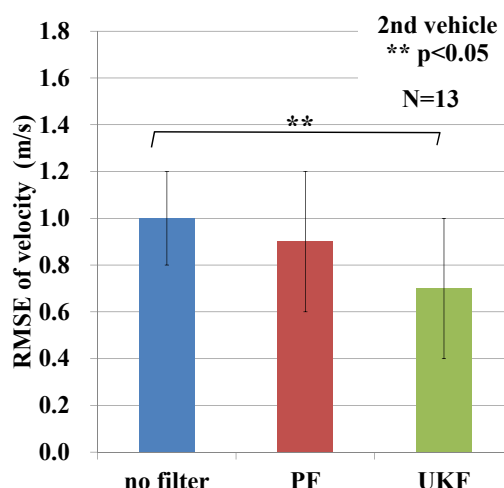


Figure 18. RMSE of velocity estimations (measuring acceleration and velocity)

### Concluding Remarks

This research applied both the PF and the UKF to the state estimation of vehicle platooning, instead of conventional approaches such as the EKF or the NKF. Headway distance and the velocity of a three-vehicle platoon were estimated by observing the acceleration rate and/or velocity of the third vehicle as a probe car. The particles or sigma points generated through the PF and UKF are expected to capture the posterior mean and covariance of the true state variables to yield a more accurate estimate than the EKF and NKF.

Numerical analyses using artificial car-following data demonstrated that the PF and NKF provided significantly and statistically higher accuracy of the estimates compared to the other estimators in both the case where only acceleration is observed and that where velocity is also measured. Not only is the error small, but also the error variance is small, so that the PF and UKF yield stable and accurate estimates in all the examined car-following cases. Even in the evaluation using real car-following data collected through a test track field test, the estimation accuracy is as low as a satisfactorily level although the estimation error is slightly larger than the case using the artificial data.

Even without equipping vehicles with costly sensors or cameras to measure the headway distance, the proposed algorithm is expected to approximate headway distance in real time. However, the significant performance of PF and UKF demonstrated here is solely limited only for the three-vehicle platoon and short time car-following. Further work should be carried out to apply the estimation to a larger platoon system and the much longer period of car-following including various acceleration and deceleration situations.

### Acknowledgment

This work was supported by JSPS KAKENHI Grant Number C24510231. The authors wish their sincere appreciation to Japan Automobile Research Institute for giving us a real data.

### References

- Hiraoka, T. Takada, S., Kawakami, H (2012) Effect of forward obstacles collision

- warning system based on deceleration for collision avoidance on driving behavior, *Proceedings of 19th World Congress on Intelligent Transport Systems*.
- Kitajima, S., Marumo, Y., Hiraoka, T., Itoh, M. (2009) Comparison of evaluation indices concerning estimation of driver's risk perception of rear-end collision to a preceding vehicle-, *Transactions of JSAE*, 40(2), 597–602. (in Japanese).
- Galler, B. A., Asher, H. (1995) Vehicle-to-vehicle communication for collision avoidance and improved traffic flow, *IDEA Project Final Report Contract*, ITS-1, Transportation Research Board.
- Biswas, S., Tatchikou, R., Dion, F. (2006) Vehicle-to-vehicle wireless communication protocols for enhancing highway traffic safety, *Communications Magazine*, IEEE, 44(1), 74-82.
- Gechter, F., Contet, J-M., Lamotte, O., Galland, S., Koukam, A. (2012) Virtual intelligent vehicle urban simulator: application to vehicle platoon evaluation, *Journal of Simulation Modeling Practice and Theory*, 2012.
- Contet, J-M, Gechter, F., Gruer, J-P., Koukam, A. (2007) Application of reactive multiagent system to linear vehicle platoon, *19th IEEE International Conference on Tools with Artificial Intelligence – ICTAI'2007*, IEEE Computer Society, Vol.2, 67-70.
- Yi, S-Y., Chong, K-T. (2005) Impedance control for a vehicle platoon system, *Mechatronics*, 15(5), 627-638, Elsevier.
- Suzuki, H., Fujii, T., Fukushima, M. (2011) Safety analysis of passenger car and heavy-vehicle mixed platoon on real-world arterial corridor using car-following simulation, *Transactions of JSAE*, 42(4), 961–966. (in Japanese)
- Farrelly, J. Wellstead, P. (1996) Estimation of vehicle lateral velocity, *Proceedings of the 1996 IEEE International Conference on Control Applications*, 552- 557.
- Suzuki, H., Nakatsuji, T. (2011) Dynamic estimation of velocity and spacing between vehicles using Neural Kalman filter, *the 21st Annual Conference of the Japanese Neural Network Society*.
- Suzuki, H. (2012) Dynamic estimation of velocity and headway distance of longitudinal platooning vehicles using neural Kalman filter, *Transactions of the Society of Instrument and Control Engineers*, 48 (11), 781–789. (in Japanese)
- Papageorgiou, M. et al. (1989) Macroscopic modeling of traffic flow on the Boulevard Peripherique in Paris, *Transportation Research-B*, 23B(1), 29–47.
- Rothery R. W. (1998) Car following models (Chapter 4). In: Gartner N, Messer C J, Rathi A K, editors. Revised monograph on traffic flow theory, FHWA.
- Pourmoallem, N., Nakatsuji, T., Kawamura, A. (1997) A Neural-Kalman filtering method for estimating traffic states on freeways, *Journal of Infrastructure Planning and Management*, JSCE, 569-IV36, 105–114.
- Kobayashi, T (2012) Dual estimations of traffic states and parameters, Master Thesis of Hokkaido University. (in Japanese)  
(<http://www.eng.hokudai.ac.jp/labo/tra/jp/doc/Thesis/H23/2011.23.Kobayashi.pdf>)
- Nishiyama, K. (2011) Kalman filter (Chapter 6), *The Knowledge Base*, The Institute of Electronics, Information and Communication Engineers, 23pp. (in Japanese)
- Haykin, S. (2001) Kalman filtering and neural networks, John Wiley & Sons, 304pp.
- Ikoma, N. (2012) Sequential Monte Carlo method and particle filter, Chapter 11, Vol. III, *Statistical Science of 21 Century*, HP edition, Japan Statistical Society (in Japanese)
- Arulampalam, M. S., Maskell, S., Gordon, N. and Clapp, T. (2002) A tutorial on particle filters for online nonlinear/non-gaussian Bayesian tracking, *IEEE Transactions on Signal Processing*, 50(2), 174-188.